Power Flow Study and Comparison of FACTS: Series (SSSC), Shunt (STATCOM), and Shunt-Series (UPFC).

Alireza Seifi, Ph.D.[*]; Sasan Gholami, M.S.; and Amin Shabanpour, M.S.

Department of Power and Control, Faculty of Electrical and Computer Engineering,
Shiraz University, Shiraz, Iran.

[*]E-mail: seifi@shirazu.ac.ir

ABSTRACT

This paper presents an AC Transmission system power flow controlled by injecting a compensating voltage in series with the line and injecting reactive power in shunt with the bus. Static Synchronous Series Compensator (SSSC) and Static Synchronous Compensator (STATCOM) are utilized as a series and shunt compensation, respectively while Unified Power Flow Controller (UPFC) is considered as a shunt-series compensator. This paper covers, in depth, the modeling and simulation methods required for a thorough study of the steady-state operation of electrical power systems with these flexible AC Transmission Systems (FACTS) controllers. A thorough grounding on the theory and practice of positive sequence power flow is offered here. MATLAB® codes are utilized for the implementation of the three devices in the Newton-Raphson algorithm. Power flow control ranges are evaluated for standard 14-bus system. Results are reported and studies are presented to illustrate and compare the effectiveness of the STATCOM, SSSC and UPFC.

(Keywords: FACTS, flexible AC transmission systems, MATLAB, Newton-Raphson algorithm, power flow, Static Synchronous Compensator, STATCOM, Static Synchronous Series Compensator, SSSC, Unified Power Flow Controller, UPFC)

INTRODUCTION

With regards to the deregulation of the power system industry and higher industrial demands, transmission facilities are being excessively used. This provides the need for building new transmission lines and electricity generating plants, a solution that is costly to implement and that involves long construction times and opposition from pressure groups. So other ways of maximizing the power transfers of existing transmission facilities while simultaneously maintaining acceptable levels of network reliability and stability should be considered.

Recent advancements in power electronics have proven to satisfy this need by introducing the concept of flexible AC transmission system (FACTS). FACTS-devices can be utilized to increase the transmission capacity, improve the stability and dynamic behavior or ensure better power quality in modern power systems. Their main capabilities are reactive power compensation, voltage control, and power flow control [4]. Due to their controllable power electronics, FACTS-devices always provide fast control actions in comparison to conventional devices like switched compensation or phase shifting transformers with mechanical on-load tap changers.

The first generation of FACTS-devices was mechanically controlled capacitors and inductors. The second generation of FACTS devices replaced the mechanical switches by the thyristor valve control. The second generation gave a noticeable improvement in the speed and the enhancement in concept to mitigate the disturbances. The third generation uses the concept of voltage source converter based devices. These devices provide multi-dimensional control of the power system parameters [7], [8].

It is well known that power flow calculations are the most frequently performed routine power network calculations, which can be used in power system planning, operational planning, and operation/control. It is also considered as the fundamental of power system network calculations. The calculations are required for the analysis of steady-state as well as dynamic performance of power systems. Among the power flow methods proposed, the Newton's method technique [2] has been considered as the power

flow solution technique for large-scale power system analysis. A detailed review of power flow methods can be found in [4]. This paper deals with the steady state models of STATCOM [1], [4] SSSC [9], [10], and UPFC [1], [4], [8] which can be combined in Newton-Raphson load flow algorithm.

POWER FLOW CONTROL

The power transmission line can be represented by a two-bus system "k" and "m" in ordinary form [6]. The active power transmitted betweens bus nodes k and m is given by:

$$P = \frac{V_m * V_k}{X} \sin(\delta_k - \delta_m) \quad (1)$$

Where V_k and V_m are the voltages at the nodes, $(\delta_k - \delta_m)$ the angle between the voltages and X, the line impedance. The power flow can be controlled by altering the voltages at a node, the impedance between the nodes and the angle between the end voltages. The reactive power is given by:

$$Q = \frac{V_k^2}{X} - \frac{V_m * V_k}{X} \cos(\delta_k - \delta_m) \quad (2)$$

NEWTON-RAPHSON POWER FLOW

In large-scale power flow studies, the Newton-Raphson [8] has proved most successful owing to its strong convergence characteristics. The power flow Newton-Raphson algorithm is expressed by the following relationship:

$$\begin{bmatrix} \Delta P \\ \Delta Q \end{bmatrix} = \begin{bmatrix} \frac{\partial P}{\partial \theta} & v\frac{\partial P}{\partial v} \\ \frac{\partial Q}{\partial \theta} & v\frac{\partial Q}{\partial v} \end{bmatrix} \begin{bmatrix} \Delta\theta \\ \frac{\Delta v}{v} \end{bmatrix} \quad (3)$$

Where **ΔP** and **ΔQ** are bus active and reactive power mismatches, while **θ** and **V** are bus magnitude and angle, respectively.

MODELING OF POWER SYSTEMS WITH STATCOM

It is acceptable to expect that for the aim of positive sequence power flow analysis the STATCOM will be represented by a synchronous voltage source with maximum and minimum voltage magnitude limits [4]. The synchronous voltage source stands for the fundamental Fourier series component of the switched voltage waveform at the AC converter terminal of the STATCOM. The bus at which the STATCOM is connected is represented as a PV bus, which may change to a PQ bus in the case of limits being violated. In this case, the generated or absorbed reactive power would reach to the maximum limit. The STATCOM equivalent circuit shown in Figure 1 is used to obtain the mathematical model of the controller for incorporation in power flow algorithms [2].

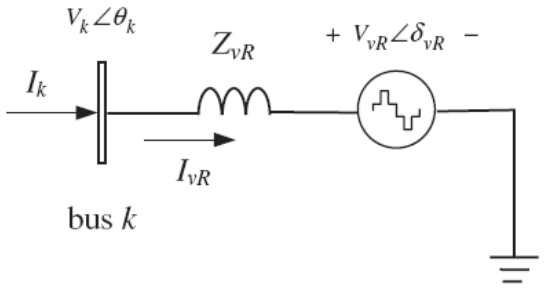

Figure 1: STATCOM Equivalent Circuit.

The power flow equations for the STATCOM are derived below:

$$E_{vR} = V_{vR}(\cos\delta_{vR} + j\sin\delta_{vR}) \quad (4)$$

Based on the shunt connection shown in Figure 1, the following may be written:

$$S_{vR} = V_{vR} I_{vR}^* = V_{vR} Y_{vR}^* (V_{vR}^* - V_k^*) \quad (5)$$

After performing some complex operations, the following active and reactive power equations are obtained for the converter and bus k, respectively:

$$P_{vR} = V_{vR}^2 G_{vR} + V_{vR} V_k [G_{vR} \cos(\delta_{vR} - \theta_k) + B_{vR} \sin(\delta_{vR} - \theta_k)] \quad (6)$$

$$Q_{vR} = -V_{vR}^2 B_{vR} + V_{vR} V_k [G_{vR} \sin(\delta_{vR} - \theta_k) - B_{vR} \cos(\delta_{vR} - \theta_k)] \quad (7)$$

$$P_k = V_k^2 G_{vR} + V_k V_{vR}[G_{vR}\cos(\theta_k - \delta_{vR}) + B_{vR}\sin(\theta_k - \delta_{vR})] \quad (8)$$

$$Q_k = -V_k^2 B_{vR} + V_k V_{vR}[G_{vR}\sin(\theta_k - \delta_{vR}) - B_{vR}\cos(\theta_k - \delta_{vR})] \quad (9)$$

Using these power equations, the linearized STATCOM model is given below, where the voltage magnitude V_{vR} and phase angle δ_{vR} are taken to be the state variables [4]:

$$\begin{bmatrix} \Delta P_k \\ \Delta Q_k \\ \Delta P_{vR} \\ \Delta Q_{vR} \end{bmatrix} = \begin{bmatrix} \frac{\partial P_k}{\partial \theta_k} & \frac{\partial P_k}{\partial V_k}V_k & \frac{\partial P_k}{\partial \delta_{vR}} & \frac{\partial P_k}{\partial V_{vR}}V_{vR} \\ \frac{\partial Q_k}{\partial \theta_k} & \frac{\partial Q_k}{\partial V_k}V_k & \frac{\partial Q_k}{\partial \delta_{vR}} & \frac{\partial Q_k}{\partial V_{vR}}V_{vR} \\ \frac{\partial P_{vR}}{\partial \theta_k} & \frac{\partial P_{vR}}{\partial V_k}V_k & \frac{\partial P_{vR}}{\partial \delta_{vR}} & \frac{\partial P_{vR}}{\partial V_{vR}}V_{vR} \\ \frac{\partial Q_{vR}}{\partial \theta_k} & \frac{\partial Q_{vR}}{\partial V_k}V_k & \frac{\partial Q_{vR}}{\partial \delta_{vR}} & \frac{\partial Q_{vR}}{\partial V_{vR}}V_{vR} \end{bmatrix} \begin{bmatrix} \Delta\theta_k \\ \frac{\Delta V_k}{V_k} \\ \Delta\delta_{vR} \\ \frac{\Delta V_{vR}}{V_{vR}} \end{bmatrix} \quad (10)$$

MODELING OF POWER SYSTEMS WITH SSSC

Figure 2 shows the circuit model of an SSSC connected to link k–m. The objective for the addition of SSSC is to control the active power P_k to a target value [10]. The SSSC is modeled as a voltage source (V_{cR}) with adjustable magnitude and angle in series with an impedance. The real part of this impedance represents the ohmic losses of the power electronic devices and the coupling transformer. The imaginary part of this impedance represents the leakage reactance of the coupling transformer. The admittance Y_s shown in Figure 2 represents the combined admittances of the SSSC and the line to which it is connected [9]. The presence of V_{cR} introduces two new variables ($|V_{cR}|$ and δ_{cR}) to the power flow problem. Thus, two new equations are needed for power flow solution. One of these equations is found by equating P_k to its target value, and the other one is found using the fact that the power consumed by the source V_{cR} is equal to zero. The power flow equations for all buses of the power system with SSSC in place are the same as those of the system without SSSC, except for Buses k and m [8].

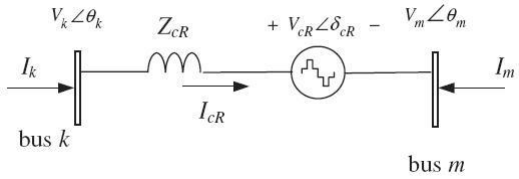

Figure 2: SSSC Equivalent Circuit.

The SSSC voltage source is:

$$E_{cR} = V_{cR}(\cos\delta_{cR} + j\sin\delta_{cR}) \quad (11)$$

The magnitude V_{cR} and phase angle δ_{cR} of the voltage source representing the series converter are controlled between limits ($V_{cR,min} \le V_{cR} \le V_{cR,max}$) and ($0 \le \delta_{cR} \le 2\pi$), respectively. Based on the equivalent circuit shown in Figure 2 and Equations (11), the active and reactive power equations at bus k are:

$$P_k = V_k^2 G_{kk} + V_k V_m[G_{km}\cos(\theta_k - \theta_m) + B_{km}\sin(\theta_k - \theta_m)] + V_k V_{cR}[G_{km}\cos(\theta_k - \delta_{cR}) + B_{km}\sin(\theta_k - \delta_{cR})] \quad (12)$$

$$Q_k = -V_k^2 B_{kk} + V_k V_m[G_{km}\sin(\theta_k - \theta_m) - B_{km}\cos(\theta_k - \theta_m)] + V_k V_{cR}[G_{km}\sin(\theta_k - \delta_{cR}) - B_{km}\cos(\theta_k - \delta_{cR})] \quad (13)$$

And for series converter are:

$$P_{cR} = V_{cR}^2 G_{mm} + V_{cR} V_k[G_{km}\cos(\delta_{cR} - \theta_k) + B_{km}\sin(\delta_{cR} - \theta_k)] + V_{cR} V_m[G_{mm}\cos(\delta_{cR} - \theta_m) + B_{mm}\sin(\delta_{cR} - \theta_m)] \quad (14)$$

$$Q_{cR} = -V_{cR}^2 B_{mm} + V_{cR} V_k[G_{km}\sin(\delta_{cR} - \theta_k) - B_{km}\cos(\delta_{cR} - \theta_k)] + V_{cR} V_m[G_{mm}\sin(\delta_{cR} - \theta_m) - B_{mm}\cos(\delta_{cR} - \theta_m)] \quad (15)$$

The system of equations is as follows:

$$\begin{bmatrix} \Delta P_k \\ \Delta P_m \\ \Delta Q_k \\ \Delta Q_m \\ \Delta P_{mk} \\ \Delta Q_{mk} \end{bmatrix} = \begin{bmatrix} \frac{\partial P_k}{\partial \theta_k} & \frac{\partial P_k}{\partial \theta_m} & \frac{\partial P_k}{\partial V_k}V_k & \frac{\partial P_k}{\partial V_m}V_m & \frac{\partial P_k}{\partial \delta_{cR}} & \frac{\partial P_k}{\partial V_{cR}}V_{cR} \\ \frac{\partial P_m}{\partial \theta_k} & \frac{\partial P_m}{\partial \theta_m} & \frac{\partial P_m}{\partial V_k}V_k & \frac{\partial P_m}{\partial V_m}V_m & \frac{\partial P_m}{\partial \delta_{cR}} & \frac{\partial P_m}{\partial V_{cR}}V_{cR} \\ \frac{\partial Q_k}{\partial \theta_k} & \frac{\partial Q_k}{\partial \theta_m} & \frac{\partial Q_k}{\partial V_k}V_k & \frac{\partial Q_k}{\partial V_m}V_m & \frac{\partial Q_k}{\partial \delta_{cR}} & \frac{\partial Q_k}{\partial V_{cR}}V_{cR} \\ \frac{\partial Q_m}{\partial \theta_k} & \frac{\partial Q_m}{\partial \theta_m} & \frac{\partial Q_m}{\partial V_k}V_k & \frac{\partial Q_m}{\partial V_m}V_m & \frac{\partial Q_m}{\partial \delta_{cR}} & \frac{\partial Q_m}{\partial V_{cR}}V_{cR} \\ \frac{\partial P_{mk}}{\partial \theta_k} & \frac{\partial P_{mk}}{\partial \theta_m} & \frac{\partial P_{mk}}{\partial V_k}V_k & \frac{\partial P_{mk}}{\partial V_m}V_m & \frac{\partial P_{mk}}{\partial \delta_{cR}} & \frac{\partial P_{mk}}{\partial V_{cR}}V_{cR} \\ \frac{\partial Q_{mk}}{\partial \theta_k} & \frac{\partial Q_{mk}}{\partial \theta_m} & \frac{\partial Q_{mk}}{\partial V_k}V_k & \frac{\partial Q_{mk}}{\partial V_m}V_m & \frac{\partial Q_{mk}}{\partial \delta_{cR}} & \frac{\partial Q_{mk}}{\partial V_{cR}}V_{cR} \end{bmatrix} \begin{bmatrix} \Delta\theta_k \\ \Delta\theta_m \\ \frac{\Delta V_k}{V_k} \\ \frac{\Delta V_m}{V_m} \\ \Delta\delta_{cR} \\ \frac{\Delta V_{cR}}{V_{cR}} \end{bmatrix}$$

(**16**)

MODELING OF POWER SYSTEMS WITH UPFC

For the purpose of fundamental frequency steady-state analysis an equivalent circuit consisting of two coordinated synchronous voltage sources should represent the UPFC adequately. Such an equivalent circuit is shown in Figure 3. The synchronous voltage sources represent the fundamental Fourier series component of the switched voltage waveforms at the AC converter terminals of the UPFC [7].

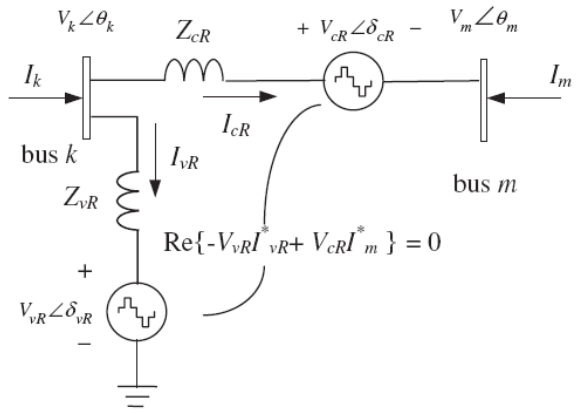

Figure 3: UPFC Equivalent Circuit.

The UPFC voltage sources are:

$$\boldsymbol{E_{vR} = V_{vR}(\cos\delta_{vR} + j\sin\delta_{vR})} \quad (\mathbf{17})$$

$$\boldsymbol{E_{cR} = V_{cR}(\cos\delta_{cR} + j\sin\delta_{cR})} \quad (\mathbf{18})$$

Where V_{vR} and δ_{vR} are the controllable magnitude ($V_{vR,min} \le V_{vR} \le V_{vR,max}$) and phase angle ($0 \le \delta_{vR} \le 2\pi$) of the voltage source representing the shunt converter. The magnitude V_{cR} and phase angle δ_{cR} of the voltage source representing the series converter are controlled between limits ($V_{cR,min} \le V_{cR} \le V_{cR,max}$) and ($0 \le \delta_{cR} \le 2\pi$), respectively. The phase angle of the series-injected voltage determines the mode of power flow control. If δ_{cR} is in phase with the nodal voltage angle θ_k, the UPFC regulates the terminal voltage. If δ_{cR} is in quadature with respect to θ_k, it controls active power flow, acting as a phase shifter. If δ_{cR} is in quadrature with the line current angle then it controls active power flow, acting as a variable series compensator [3]. At any other value of δ_{cR}, the UPFC operates as a combination of voltage regulator, variable series compensator, and phase shifter. The magnitude of the series-injected voltage determines the amount of power flow to be controlled.

Based on the equivalent circuit shown in Figure 3 and Equations (17) and (18), the active and reactive power equations are at bus k [4]:

$$\begin{aligned} P_k = {} & V_k^2 G_{kk} + V_k V_m [G_{km}\cos(\theta_k - \theta_m) \\ & + B_{km}\sin(\theta_k - \theta_m)] + V_k V_{cR}[G_{km}\cos(\theta_k - \delta_{cR}) \\ & + B_{km}\sin(\theta_k - \delta_{cR})] + V_k V_{vR}[G_{vR}\cos(\theta_k - \delta_{vR}) \\ & + B_{vR}\sin(\theta_k - \delta_{vR})] \end{aligned} \quad (\mathbf{19})$$

$$\begin{aligned} Q_k = {} & -V_k^2 B_{kk} + V_k V_m [G_{km}\sin(\theta_k - \theta_m) \\ & - B_{km}\cos(\theta_k - \theta_m)] + V_k V_{cR}[G_{km}\sin(\theta_k - \delta_{cR}) \\ & - B_{km}\cos(\theta_k - \delta_{cR})] + V_k V_{vR}[G_{vR}\sin(\theta_k - \delta_{vR}) \\ & - B_{vR}\cos(\theta_k - \delta_{vR})] \end{aligned} \quad (\mathbf{20})$$

At bus m:

$$\begin{aligned} P_k = {} & V_m^2 G_{mm} + V_m V_k [G_{mk}\cos(\theta_m - \theta_k) \\ & + B_{mk}\sin(\theta_m - \theta_k)] + \\ & V_m V_{cR}[G_{mm}\cos(\theta_m - \delta_{cR}) + \\ & B_{mm}\sin(\theta_m - \delta_{cR})] \end{aligned} \quad (\mathbf{21})$$

$$\begin{aligned} Q_k = {} & -V_m^2 B_{mm} + V_m V_k [G_{mk}\sin(\theta_m - \theta_k) \\ & - B_{mk}\cos(\theta_m - \theta_k)] + \\ & V_m V_{cR}[G_{mm}\sin(\theta_m - \delta_{cR}) - \\ & B_{mm}\cos(\theta_m - \delta_{cR})] \end{aligned} \quad (\mathbf{22})$$

Series converter:

$$P_{cR} = V_{cR}^2 G_{mm} + V_{cR} V_k [G_{km} \cos(\delta_{cR} - \theta_k) + B_{km} \sin(\delta_{cR} - \theta_k)] + V_{cR} V_m [G_{mm} \cos(\delta_{cR} - \theta_m) + B_{mm} \sin(\delta_{cR} - \theta_m)] \quad (23)$$

$$Q_{cR} = -V_{cR}^2 B_{mm} + V_{cR} V_k [G_{km} \sin(\delta_{cR} - \theta_k) - B_{km} \cos(\delta_{cR} - \theta_k)] + V_{cR} V_m [G_{mm} \sin(\delta_{cR} - \theta_m) - B_{mm} \cos(\delta_{cR} - \theta_m)] \quad (24)$$

Shunt converter:

$$P_{vR} = -V_{vR}^2 G_{vR} + V_{vR} V_k [G_{vR} \cos(\delta_{vR} - \theta_k) + B_{vR} \sin(\delta_{vR} - \theta_k)] \quad (25)$$

$$Q_{vR} = V_{vR}^2 B_{vR} + V_{vR} V_k [G_{vR} \sin(\delta_{vR} - \theta_k) - B_{vR} \cos(\delta_{vR} - \theta_k)] \quad (26)$$

The UPFC power equations, in linearized form, are combined with those of the AC network. For the case when the UPFC controls the following parameters:

(1) Voltage magnitude at the shunt converter terminal (bus k),
(2) Active power flow from bus m to bus k,
(3) Reactive power injected at bus m, and taking bus m to be a PQ bus.

The linearized system of equation is as follows [4]:

$$\begin{bmatrix} \Delta P_k \\ \Delta P_m \\ \Delta Q_k \\ \Delta Q_m \\ \Delta P_{mk} \\ \Delta Q_{mk} \\ \Delta P_{bb} \end{bmatrix} = \begin{bmatrix} \frac{\partial P_k}{\partial \theta_k} & \frac{\partial P_k}{\partial \theta_m} & \frac{\partial P_k}{\partial V_{vR}} V_{vR} & \frac{\partial P_k}{\partial V_m} V_m & \frac{\partial P_k}{\partial \delta_{cR}} & \frac{\partial P_k}{\partial V_{cR}} V_{cR} & \frac{\partial P_k}{\partial \delta_{vR}} \\ \frac{\partial P_m}{\partial \theta_k} & \frac{\partial P_m}{\partial \theta_m} & 0 & \frac{\partial P_m}{\partial V_m} V_m & \frac{\partial P_m}{\partial \delta_{cR}} & \frac{\partial P_m}{\partial V_{cR}} V_{cR} & 0 \\ \frac{\partial Q_k}{\partial \theta_k} & \frac{\partial Q_k}{\partial \theta_m} & \frac{\partial Q_k}{\partial V_{vR}} V_{vR} & \frac{\partial Q_k}{\partial V_m} V_m & \frac{\partial Q_k}{\partial \delta_{cR}} & \frac{\partial Q_k}{\partial V_{cR}} V_{cR} & \frac{\partial Q_k}{\partial \delta_{vR}} \\ \frac{\partial Q_m}{\partial \theta_k} & \frac{\partial Q_m}{\partial \theta_m} & 0 & \frac{\partial Q_m}{\partial V_m} V_m & \frac{\partial Q_m}{\partial \delta_{cR}} & \frac{\partial Q_m}{\partial V_{cR}} V_{cR} & 0 \\ \frac{\partial P_{mk}}{\partial \theta_k} & \frac{\partial P_{mk}}{\partial \theta_m} & 0 & \frac{\partial P_{mk}}{\partial V_m} V_m & \frac{\partial P_{mk}}{\partial \delta_{cR}} & \frac{\partial P_{mk}}{\partial V_{cR}} V_{cR} & 0 \\ \frac{\partial Q_{mk}}{\partial \theta_k} & \frac{\partial Q_{mk}}{\partial \theta_m} & 0 & \frac{\partial Q_{mk}}{\partial V_m} V_m & \frac{\partial Q_{mk}}{\partial \delta_{cR}} & \frac{\partial Q_{mk}}{\partial V_{cR}} V_{cR} & 0 \\ \frac{\partial P_{bb}}{\partial \theta_k} & \frac{\partial P_{bb}}{\partial \theta_m} & \frac{\partial P_{bb}}{\partial V_{vR}} V_{vR} & \frac{\partial P_{bb}}{\partial V_m} V_m & \frac{\partial P_{bb}}{\partial \delta_{cR}} & \frac{\partial P_{bb}}{\partial V_{cR}} V_{cR} & \frac{\partial P_{bb}}{\partial \delta_{vR}} \end{bmatrix} \begin{bmatrix} \Delta\theta_k \\ \Delta\theta_m \\ \frac{\Delta V_{vR}}{V_{vR}} \\ \frac{\Delta V_m}{V_m} \\ \Delta\delta_{cR} \\ \frac{\Delta V_{cR}}{V_{cR}} \\ \Delta\delta_{vR} \end{bmatrix} \quad (27)$$

TEST CASE AND SIMULATION

Standard 14-bus test network is tested with STATCOM, SSSC and UPFC separately, to investigate the behavior of the two devices in the network.

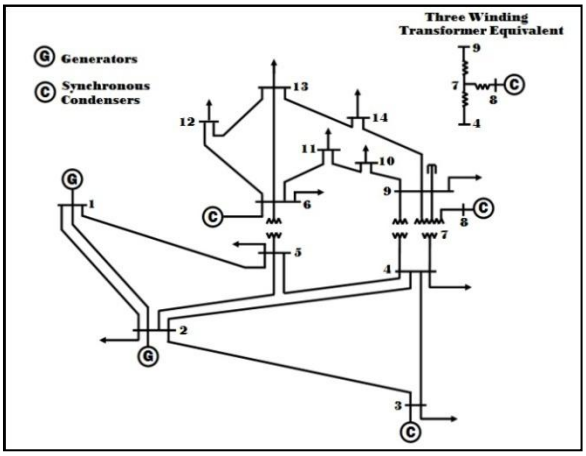

Figure 4: Standard 14-bus Network.

Power flow program is executed for 4 cases. The first case is the base case, without inserting any FACTS-devices. Other Cases are the same network with the addition of STATCOM, SSSC and UPFC, respectively. The results of power flow without using any FACTS are outlined in Table 1.

The 14-bus network is modified to include one STATCOM connected at bus 14, to maintain the nodal voltage magnitude at 1.04 p.u. The power flow solution is shown in Tables 2a and 2b whereas the nodal voltage magnitudes and phase angles are given. Convergence is achieved in four iterations to a power mismatch tolerance of 10^{-4}.

The power flow result indicates that the STATCOM generates 0.2383 MVAR in order to keep the voltage magnitude at 1.04 p.u. at bus 14. Use of the STATCOM results in an improved network voltage profile. The slack generator increases its reactive power absorption by almost 2.6% compared with the base case, and the direction of reactive power from bus 14 to bus 13 has been changed. The largest reactive power flow takes place in the transmission line connecting bus 1 and bus 2, which is 0.3794 p.u.

Table 1a: Power flow without FACTS: Bus Results.

Bus no.	Voltage (|V|,θ)	Load (MW,Mvar) pu	Generator (MW,Mvar) pu
1	1.06, 0	0,0	3.5205, -0.2789
2	1.045, -0.1355	0.3038, 0.1778	0.4, 0.9513
3	1.01, -0.3316	1.3188, 0.266	0, 0.5979
4	0.9977, -0.2634	0.6692, 0.056	0,0
5	1.0024, -0.2278	0.1064, 0.0224	0,0
6	1.07, -0.3795	0.1568, 0.105	0, 0.4426
7	1.0347, -0.3539	0,0	0,0
8	1.09, -0.3539	0,0	0, 0.3424
9	1.0111, -0.4018	0.413, 0.2324	0,0
10	1.0105, -0.4049	0.126, 0.0812	0,0
11	1.0346, -0.3950	0.049, 0.0252	0,0
12	1.0461, -0.4014	0.0854, 0.0224	0,0
13	1.0362, -0.4031	0.189, 0.0812	0,0
14	0.9957, -0.4285	0.2086, 0.07	0,0

Table 2a: Power flow with STATCOM: Bus Results.

Bus no.	Voltage (|V|,θ)	Load (MW,Mvar) pu	Generator (MW,Mvar) pu
1	1.06,0	0,0	3.518, -0.2864
2	1.045, -0.1354	0.3038, 0.1778	0.4, 0.9263
3	1.01, -0.3312	1.3188, 0.266	0, 0.5827
4	1.001, -0.2640	0.6692, 0.056	0,0
5	1.0041, -0.2274	0.1064, 0.0224	0,0
6	1.07, -0.3766	0.1568, 0.105	0, 0.2869
7	1.0427, -0.3551	0,0	0,0
8	1.09, -0.3551	0,0	0, 0.2926
9	1.0271, -0.4028	0.413, 0.2324	0,0
10	1.0238, -0.4052	0.126, 0.0812	0,0
11	1.0414, -0.3939	0.049, 0.0252	0,0
12	1.0521, -0.3997	0.0854, 0.0224	0,0
13	1.0473, -0.4050	0.189, 0.0812	0,0
14	1.045, -0.4444	0.2086, 0.07	0, 0.2383

Table 1b: Power flow without FACTS: Line Results.

Line no.	From Bus / To Bus	Power Flow	
		P , pu	Q , pu
1	2-5	0.5827	0.0722
2	6-12	0.1172	0.0446
3	12-13	0.0301	0.0187
4	6-13	0.2731	0.1416
5	6-11	0.1444	0.1219
6	11-10	0.0925	0.0905
7	9-10	0.0384	-0.0062
8	9-14	0.104	0.0100
9	14-13	-0.1059	-0.0628
10	7-9	0.4558	0.2326
11	1-2	2.415	-0.3802
12	3-2	-1.000	0.1386
13	3-4	-0.3184	0.1933
14	1-5	1.105	0.1012
15	5-4	0.8125	-0.1383
16	2-4	0.7780	0.0516
17	5-6	0.0959	0.0359
18	4-9	0.6916	0.0761
19	4-7	0.4558	-0.0500
20	8-7	0	0.3424

Table 2b: Power flow with STATCOM: Line Results.

Line no.	From Bus / To Bus	Power Flow	
		P , pu	Q , pu
1	2-5	0.5811	0.0627
2	6-12	0.1124	0.0220
3	12-13	0.0256	-0.0032
4	6-13	0.2712	0.0519
5	6-11	0.1390	0.0882
6	11-10	0.0878	0.0583
7	9-10	0.0391	0.0250
8	9-14	0.1102	-0.1164
9	14-13	-0.1014	0.0452
10	7-9	0.4640	0.1592
11	1-2	2.412	-0.3794
12	3-2	-0.9990	0.1381
13	3-4	-0.3197	0.1786
14	1-5	1.105	0.0933
15	5-4	0.8231	-0.1604
16	2-4	0.7791	0.0370
17	5-6	0.0983	0.0112
18	4-9	0.6796	0.0820
19	4-7	0.4640	-0.0765
20	8-7	0	0.2926

The result value of the STATCOM voltage source is taken to be $V_{vR} = 1.04$ p.u. In general, more reactive power is available in the network than in the base case, and the generator connected at bus 1 increases its share of reactive power absorption compared with the base case.

The original 14-bus network is modified to include one SSSC to compensate the transmission line connected between bus14 and bus13. The SSSC is used to increase active power flowing from bus 14 towards bus 13 by 50% line compensation. Convergence is obtained in 4 iterations to a power mismatch tolerance of 10^{-4}. The power flow results are shown in Tables 3 a and b.

Table 3a: Power flow with SSSC: Bus Results.

Bus no.	Voltage (|V|,θ)	Load (MW,Mvar) pu	Generator (MW,Mvar) pu
1	1.06,0	0,0	3.517, -0.2809
2	1.045, -0.1354	0.3038, 0.1778	0.4, 0.9414
3	1.01, -0.3316	1.3188, 0.266	0, 0.5919
4	0.9987, -0.2632	0.6692, 0.056	0,0
5	1.003, -0.2275	0.1064, 0.0224	0,0
6	1.07, -0.3808	0.1568, 0.105	0, 0.4721
7	1.0376, -0.3523	0,0	0,0
8	1.09, -0.3524	0,0	0, 0.3243
9	1.0167, -0.3994	0.413, 0.2324	0,0
10	1.0153, -0.4031	0.126, 0.0812	0,0
11	1.0371, -0.3949	0.049, 0.0252	0,0
12	1.0438, -0.4030	0.0854, 0.0224	0,0
13	1.0315, -0.4042	0.189, 0.0812	0,0
14	1.0141, -0.4250	0.2086, 0.07	0,0

As expected, nodal voltage magnitudes do not change considerably compared with the base case. The result value of the SSSC voltage source is taken to be $V_{cR} = 0.028$ p.u.

Table 3b: Power flow with SSSC: Line Results.

Line no.	From Bus / To Bus	Power Flow	
		P , pu	Q , pu
1	2-5	0.5828	0.0690
2	6-12	0.1220	0.0520
3	12-13	0.0347	0.0257
4	6-13	0.2862	0.1732
5	6-11	0.1327	0.1139
6	11-10	0.0812	0.0834
7	9-10	0.0458	0.0003
8	9-14	0.0844	-0.0283
9	14-13	-0.1251	-0.1003
10	7-9	0.4509	0.2073
11	1-2	2.412	-0.3796
12	3-2	-0.9990	0.1380
13	3-4	-0.3197	0.1878
14	1-5	1.105	0.0986
15	5-4	0.8063	-0.1472
16	2-4	0.7766	0.0462
17	5-6	0.0923	0.0272
18	4-9	0.6978	0.0795
19	4-7	0.4509	-0.0599
20	8-7	0	0.3243

The 14-bus network is modified to include one UPFC to compensate the transmission line linking bus 14 and bus 13. The UPFC is caused to maintain active and reactive powers leaving the UPFC, towards bus 14, at -0.1322 p.u. and 0.0148 p.u, respectively. Moreover, the UPFC shunt converter is set to regulate the nodal voltage magnitude at bus 14 at 1.04 p.u. The result values of the UPFC voltage sources are taken to be $V_{vR} = 1.04$ p.u., $V_{cR} = 0.02$ p.u. Convergence is obtained in four iterations to a power mismatch tolerance of 10^{-4}. The power flow results are shown in Tables 4 a and b.

CONCLUSION

This paper presented the modeling and simulation methods required for study of the steady-state operation of electrical power systems with FACTS controllers: STATCOM, SSSC, and UPFC. The conventional power flow solution could systematically be modified to include multiple FACTS controllers: STATCOM, SSSC, and UPFC. It was shown that the effect of FACTS controllers on power flow can be provided by adding new entries and adjusting some existing entries in the linearized Jacobean equation of the basic system with no FACTS controllers.

Table 4a: Power flow with UPFC: Bus Results.

Bus no.	Voltage (|V|,θ)	Load (MW,Mvar) pu	Generator (MW,Mvar) pu
1	1.06,0	0,0	3.5156, -0.2853
2	1.045, -0.1353	0.3038, 0.1778	0.4, 0.9256
3	1.01, -0.3308	1.3188, 0.266	0, 0.5822
4	1.003, -0.2634	0.6692, 0.056	0,0
5	1.004, -0.2274	0.1064, 0.0224	0,0
6	1.07, -0.3801	0.1568, 0.105	0, 0.3283
7	1.0426, -0.3523	0,0	0,0
8	1.09, -0.3523	0,0	0, 0.2932
9	1.0267, -0.3988	0.413, 0.2324	0,0
10	1.0236, -0.4025	0.126, 0.0812	0,0
11	1.0414, -0.3943	0.049, 0.0252	0,0
12	1.05, -0.4043	0.0854, 0.0224	0,0
13	1.0428, -0.4098	0.189, 0.0812	0,0
14	1.045, -0.431	0.2086, 0.07	0, 0.1936

Table 4b: Power flow with UPFC: Line Results.

Line no.	From Bus / To Bus	Power Flow	
		P , pu	Q , pu
1	2-5	0.5823	0.0632
2	6-12	0.1195	0.0276
3	12-13	0.0325	0.0019
4	6-13	0.2943	0.0780
5	6-11	0.1248	0.0948
6	11-10	0.0737	0.0653
7	9-10	0.0530	0.0177
8	9-14	0.0783	-0.1044
9	14-13	-0.1322	0.0148
10	7-9	0.4526	0.1617
11	1-2	2.410	-0.3793
12	3-2	-0.9979	0.1375
13	3-4	-0.3208	0.1786
14	1-5	1.105	0.094
15	5-4	0.8083	-0.1614
16	2-4	0.7767	0.0370
17	5-6	0.0918	0.0118
18	4-9	0.6954	0.0838
19	4-7	0.4526	-0.0766
20	8-7	0	0.2932

An existing power flow program that uses the Newton–Raphson method of solution in Cartesian coordinates can easily be modified through the procedure presented in this paper. This procedure was applied on the 14-bus power system and implemented using the MATLAB® software package. The numerical results show the robust convergence of the presented procedure. The steady state models of STATCOM, SSSC, and UPFC are evaluated in Newton-Raphson algorithm and the results show that UPFC can mostly carry out the aim of both SSSC and STATCOM.

REFRENCES

1. Sahoo, A.K., S.S. Dash, and T. Thyagarajan. 2007. "\Modeling of STATCOM and UPFC for Power System Steady State Operation and Control". IET-UK International Conference on Information and Communication Technology in Electrical Sciences (ICTES 2007).

2. Gotham, D.J. and G.T. Heydt. 1998. "Power Flow Control and Power Flow Studies for Systems with FACTS Devices". *IEEE Trans. Power Syst*. 13(1): 60–66.

3. Povh, D. 2000. "Modeling of FACTS in Power System Studies". *Proc. IEEE Power Eng. Soc. Winter Meeting*. 2:1435–1439.

4. Acha, E., C.R. Fuerte-Esquivel, H. Ambriz-Pe´rez, and C. Angeles-Camacho. 2004. *FACTS: Modelling and Simulation in Power Networks*. John Wiley and Sons: West Sussex, UK.

5. Radman, G. and R.S. Raje. 2007. "Power Flow Model/Calculation for Power Systems with Multiple FACTS Controllers". *Electric Power Systems Research*. 77:1521–1531.

6. Stagg, G.W. and A.H. Ei-Abiad. 1968. *Computer Methods in Power Systems Analysis*. McGraw-Hill: New York, NY.

7. Hingorani, N.G. and L. Gyugyi. 2000. *Understanding FACTS: Concepts and Technology of Flexible AC Transmission Systems*. Wiley–IEEE Press: New York, NY. ISBN: 0-7803-3464-7.

8. Zhang, X.P., C. Rehtanz, and B. Pal. 2006. *Flexible AC Transmission Systems: Modelling and Control*. Springer Verlag: Berlin, Germany.

9. Zhang, X.P. 2003. "Advanced Modeling of Multicontrol Functional Static Synchronous Series Compensator (SSSC) in Newton–Raphson Power Flow". *IEEE Trans. Power Syst*. 18(4):1410–1416.

10. Zhang, X.P., C.F. Xue, and K.R. Godfrey. 2004. “Modelling of the Static Synchronous Series Compensator (SSSC) in Three-Phase Newton Power Flow”. *IEEE Proc.-Gener. Transm. Distrib.* 151(4).

ABOUT THE AUTHORS

Ali Reza Seifi was born in Shiraz, Iran, on August 9, 1968. He received his B.S. degree in Electrical Engineering from Shiraz University, Shiraz, Iran, in 1991, M.S. degree in Electrical Engineering from The University of Tabriz, Tabriz, Iran, in 1993, and his Ph.D. degree in Electrical Engineering from Tarbiat Modarres University (T.M.U), Tehran, Iran, in 2001, respectively. He is currently as an Associate Professor in the Department of Power and Control Engineering, School of Electrical and Computer Engineering, Shiraz University, Shiraz, Iran. His research interests are in power plant simulation, power systems, electrical machines simulation, power electronics, and fuzzy optimization.

Sasan Gholami, was born in Shiraz, Iran, on September 9, 1986. He received his B.S. degree in Electrical Engineering from Shiraz University, Shiraz, Iran, in 2008. He is currently a M.S. student in Shiraz University, Shiraz, Iran.

Amin Shabanpour, was born in Shiraz, Iran, on April 27, 1986. He received his B.S. degree in Electrical Engineering from Shiraz University, Shiraz, Iran, in 2008. He is currently a M.S. student in Shiraz University, Shiraz, Iran.

SUGGESTED CITATION

Seifi, A.R., S. Gholami, and A. Shabanpour. 2010. “Power Flow Study and Comparison of FACTS: Series (SSSC), Shunt (STATCOM), and Shunt-Series (UPFC)”. *Pacific Journal of Science and Technology*. 11(1):129-137.